Morphology and preparation of polymer dispersed liquid crystals by solvent-induced phase separation method

S. MUTLU YANIC, H. OCAK[a], F. CAKAR[a], B. BILGIN-ERAN[a], D. GUZELLER[a], O. CANKURTARAN[a,*]
Istanbul Gedik University, Department of Chemistry Technology Programme, Pendik Campus, 34906, Istanbul, Turkey
[a]Yildiz Technical University, Department of Chemistry, Davutpasa Campus, 34220, Esenler, Istanbul, Turkey

A new salicylaldimine based chiral calamitic liquid crystal 5-((S)-3,7-dimethyloctyloxy)-2-[[[4-(octyloxy) phenyl]imino]methyl]phenol (DOPIMP) has been synthesized and characterized by spectroscopic methods (^{1}H-NMR and ^{13}C-NMR). Polymer dispersed liquid crystal (PDLC) composite films were prepared from poly(methyl methacrylate) (PMMA) and DOPIMP by solvent-induced phase separation (SIPS) method. Polymer and LC composite films were controlled with ratio 20:80(wt.%LC) and 30:70(wt.%LC). The mesomorphic behavior of DOPIMP liquid crystal has been investigated by differential scanning calorimetry (DSC) and optical polarizing microscopy (PM). The mesophase of PDLC composite films were characterized by PM and the morphology of the PDLC composite films was studied using a scanning electron microscope (SEM).

(Received April 12, 2016

Keywords: Polymer dispersed liquid crystal, Composite films, Poly(methyl methacrylate)

1. Introduction

Polymer dispersed liquid crystals (PDLCs) are a-new class of materials because of their potential used in electro-optical devices ranging from switchable windows, light shutters, high resolution displays, projection light valves a so forth [1-4]. PDLC composite films are consist of micron-sized droplets of a low molecular weight liquid crystals dispersions within a polymer matrix [5]. The improving performance electro-optic properties of PDLCs are effected by a number of parameters including LC domain size, shape, density, director configuration and anchoring properties [6-7].

Most of all, the properties of nematic liquid crystal used in polymer dispersed liquid crystal films important factor to determine the electro-optical properties of PDLC composite films [8-9]. The approaches to disperse liquid crystal droplets are generally prepared by solvent-induced phase separation (SIPS), polymerization-induced phase separation (PIPS), and thermally-induced phase separation (TIPS) method [10-13]. Solvent evaporation rate plays a major role in the formulation structure of the polymer dispersed liquid crystal composite films in SIPS method. The slow evaporation rate yields bigger sized LC droplets and the fast evaporation rate gives a large number of smaller droplets [14-15]. This technique is generally used with transparent thermoplastic polymers such as PMMA.

In this study, firstly a new chiral calamitic liquid crystal 5-((S)-3,7-dimethyloctyloxy)-2-[[[4-(octyloxy) phenyl]imino]methyl]phenol (DOPIMP**)** has been synthesized and characterized. And then we have used the SIPS method where the DOPIMP and transparent polymer are dissolved in a common solvent to create a single phase. PMMA and DOPIMP were controlled with ratio 20:80 %wt. and 30:70%wt.

2. Experimental

2.1. Materials and instrumentation

PMMA was used as a acrylic polymer from Sigma-Aldrich. This is hard, rigid and transparent polymer. Toluene was purchased from Merck as a solvent.

The mesomorphic properties and dispersion of LC droplets in the polymer matrix was investigated optical polarizing microscope (PM) using a Leica Polarizing Microscope, equipped with a Metler FP-82 HT hot stage and control unit. DSC-thermograms of DOPIMP and PDLC composite films were recorded on a Perkin-Elmer DSC-6, heating and cooling rate: 10°C min^{-1} from -40 to 150 ^{0}C in a nitrogen atmosphere. The morphology of the PDLC composite films were studied using a Scanning Electron Microscope (SEM) equipped with a Zeiss EVO.

2.2. Synthesis and characterization of DOPIMP liquid crystal

The synthesis of DOPIMP was carried out as shown in Scheme 1. *(S)*-(-)-β-Citronellol was reduced to *(S)*-3,7-dimethyl-1-octanol under catalytic hydrogenation conditions (H_2, 10% Pd/C in MeOH) in the first reaction step of the DOPIMP. Then, (*S*)-3,7-Dimethyloctyl bromide was prepared from *(S)*-3,7-dimethyl-1-octanol by reaction with 48% aqu. HBr/conc. H_2SO_4 using tetrabutylammonium hydrogensulfate (TBAHS) as catalyst [16]. The aldehyde carrying (*S*)-3,7-Dimethyloctyloxy group was obtained by the reaction of 2,4-dihydroxybenzaldehyde with (*S*)-3,7-dimethyloctyl bromide, using $KHCO_3$ as base in DMF solvent. Finally, the condensation of the 4-((S)-3,7-Dimethyloctyloxy)-2-

hydroxybenzaldehyde and 4-(octyloxy)aniline in toluene using p-toluenesulfonic acid monohydrate as catalyst yields new salicylaldimine based chiral calamitic liquid crystal DOPIMP.

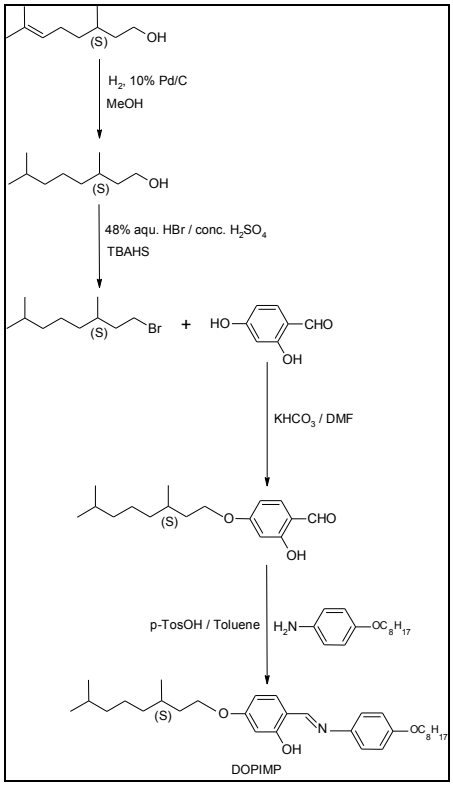

Scheme 1. Synthesis of the new salicylaldimine based chiral calamitic liquid crystal DOPIMP

The characterization of the DOPIMP is based on ^{1}H-, ^{13}C-NMR (Bruker Avance III 500 spectrometer in $CDCl_3$ solutions, with tetramethylsilane as internal standard). The proposed structure is in full agreement with the spectroscopic data.

The procedure for 5-((S)-3,7-dimethyloctyloxy)-2-[[[4-(octyloxy)phenyl]imino]methyl]phenol (DOPIMP):

Compound DOPIMP was prepared by using procedure described previously [17-20]. Into a 100 ml round-bottomed flask which was connected to the Dean-Stark apparatus, 4-(*(S)*-3,7-dimethyloctyloxy)-2-hydroxybenzaldehyde (2.5 mmol) and commercially available 4-(octyloxy)aniline (3 mmol) were dissolved in 25 ml toluene. To this solution, p-toluenesulfonic acid (40 mg) was added as catalyst and the reaction mixture was refluxed for 5h at 160 °C under argon atmosphere. The end of reaction was monitored by TLC (hexane:ethyl acetate / 10:1). After cooling, the reaction mixture was extracted into diethyl ether (3 x) and the combined organic phases were washed with saturated solution of $NaHCO_3$ and brine, respectively. The organic solution was dried over Na_2SO_4 and then removed in vacuo. The crude product was purified by recrystallization from acetone/methanol.

Yield: 73%, yellow crystals.

^{1}H-NMR (500 MHz, $CDCl_3$) δ (ppm) = 13.91 (s; OH), 8.49 (s; HC=N), 7.25-7.22 (m, 3 arom. H), 6.93 (d, J ≈ 8.9 Hz; 2 arom. H), 6.49-6.46 (m; 2 arom. H), 4.06-4.01 (m, 2H, OCH_2), 3.97 (t, J ≈ 6.6 Hz; 2H, OCH_2), 1.87-1.76 (m; 3H, CH_2, CH), 1.71-1.43, 1.39-1.14 (2m; 19H, 1 CH, 9 CH_2), 0.94 (d; *J* ≈ 6.5 Hz; 3H, CH_3), 0.90-0.86 (m, 9H, 3 CH_3).

^{13}C-NMR (125 MHz, $CDCl_3$) δ (ppm) = 163.99, 163.30, 158.57, 141.31, 113.12 (arom. C) 159.57 (HC=N), 133.73, 121.84, 115.28, 107.66, 101.61 (arom. CH), 68.39, 66.77 (OCH_2), 39.23, 37.25, 35.97, 31.92, 29.72, 29.59, 29.41, 29.34, 29.26, 24.66 (CH_2), 29.83, 27.99 (CH), 22.73, 22.63, 19.64, 14.14 (CH_3).

$C_{31}H_{47}O_3N$ (481.67); Anal. Calc.: C, 77.30; H, 9.83; N, 2.90. Found: C, 77.05; H, 9.80; N, 3.12%.

2.3. Preparation of PDLC composites films

PDLC composite films with different compositions (wt/wt.%) of PMMA and DOPIMP were prepared by SIPS method. We prepared different amounts of PMMA and DOPIMP in toluene (solvent), these solutions were stirred mechanically until glass transition temperature. LC droplets begin to form as the polymer and continue to grow until glass transition temperature of the polymer. Then mixture was dried at 50^{0}C under vacuum in order to induce the phase separation of liquid crystal droplets from the polymer matrix. PDLC composite films (PMMA:DOPIMP) were controlled with ratio (PMMA:LC) 30:70 and 20:80 wt.% [21-22].

3. Results and discussion

3.1. Liquid crystalline properties

The mesomorphic properties of the obtained the new salicylaldimine based chiral calamitic liquid crystal DOPIMP were investigated by optical polarizing microscopy (PM) and differential scanning calorimetry (DSC). The transition temperatures, corresponding enthalpy values and mesophase type observed for DOPIMP are given in Fig. 1.

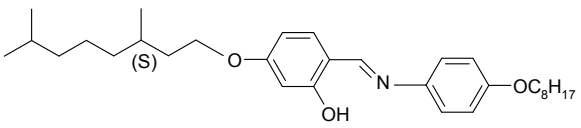

T/°C [Δ*H* kJ/mol]^{a}

Cr_1 33 [8.06] Cr_2 39 [3.55] SmC* 88 [4.44] Iso

Fig. 1. The chemical structure and phase transition temperatures of the DOPIMP [a]Perkin-Elmer DSC-6; heating /cooling rates were 10 °C min^{-1}; enthalpy values are given in square parentheses; Abbrevations: Cr = crystalline, Sm = smectic, Iso = isotropic liquid phase

The salicylaldimine based calamitic liquid crystal compound DOPIMP with an identical length of alkyl chains at both ends exhibits enantiotropic chiral smectic C* mesophase in wide temperature range. The typical textures of smectic mesophase of compound DOPIMP are shown in Fig. 2. The presence of methyl branching in the 3- and 7- position of the octyloxy chain and molecular chirality give rise to the formation of the chiral smectic phase at lower temperatures. On cooling from the isotropic liquid, broken fan-shaped texture and finger print textures of the DOPIMP were observed under the polarizing microscope as typical for SmC* phases.

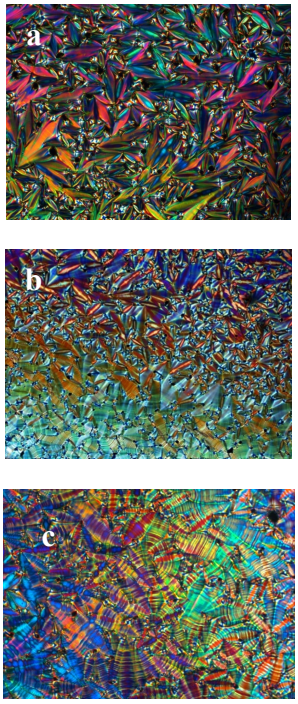

Fig. 2. The texture obtained between crossed polarizers as observed for the Smectic C phase of DOPIMP (a) texture of the SmC* phase at 78°C on cooling; (b) fan shaped texture (some region with finger print texture) of SmC* mesophase of DOPIMP at 55°C on cooling; (c) the SmC* phase at 46 °C on cooling*

3.2. PDLC composite films properties

The thermotropic behavior of polymer dispersed liquid crystal composite films were investigated by PM and DSC. As seen from DSC, the heating and cooling curves in Fig. 3 and Fig. 4 of PDLC in the ratio 20:80 (wt% LC) and 30:70 (wt% LC). Comparison of the mesomorphic properties of the DOPIMP liquid crystal with the PMMA:DOPIMP composite films show that mesophase type remains the same. As seen in DSC heating and cooling scans (see Fig. 3 and 4), the mesophase transition temperatures of the PMMA:DOPIMP composite films closely resemble to those of the DOPIMP liquid crystal. In case of the PMMA:DOPIMP composite films, the transition peak from the isotropic liquid to the LC phase is broadened. It was also found that the re-crystallization peak temperature (Tc) of 30:70 PMMA:DOPIMP (wt.%) composite film was shifted to a lower temperature and the Tc peak became broader in the DSC cooling curve.

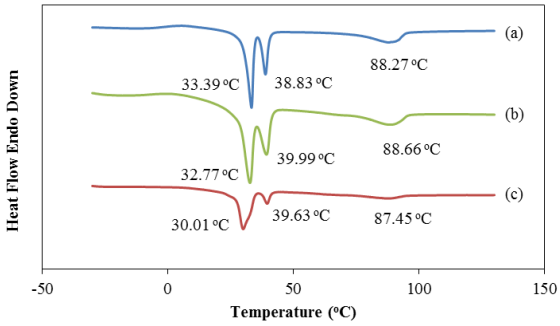

Fig. 3. DSC heating scans of (a) DOPIMP; (b) 20:80 PMMA:DOPIMP (wt%) and (c)30:70 PMMA:DOPIMP (wt%) (heating rate 10 °C min^{-1})

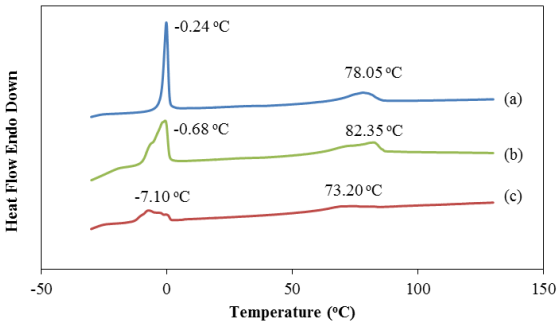

Fig. 4. DSC cooling scans of (a) DOPIMP; (b) 20:80 PMMA:DOPIMP (wt.%) and (c) 30:70 PMMA:DOPIMP (wt.%) (cooling rate 10 °C min^{-1})

The optical textures of the polymer dispersed LC in the ratio 30:70 (wt.%LC) on cooling are shown in Fig. 5. As seen from Fig. 5, optical microscopic images a homogeneous distribution of phase separated DOPIMP liquid crystal droplets was clearly seen in 30:70 (PMMA:DOPIMP) PDLC composite film. On cooling from the isotropic phase, birefringent liquid crystal droplets start appearing uniformly at 80 °C between crossed polarizers. The perfect spherical shape of liquid crystal droplets starts decomposing at 59 °C as the temperature is reduced further. The birefringent texture of SmC* mesophase texture which consists of a few randomly distributed droplets remained until 35 °C. The observed broader peaks in lower transition temperatures in DSC cooling scan of 30:70 PMMA:DOPIMP (wt.%) composite film as compared to the DOPIMP liquid crystal also confirm that the occurence of a significant change in the optical textures of the polymer dispersed LC in the ratio 30:70 (wt.%LC). This observation, together with the DSC results, indicates a liquid crystal homogenously dispersed in the polymer matrix.

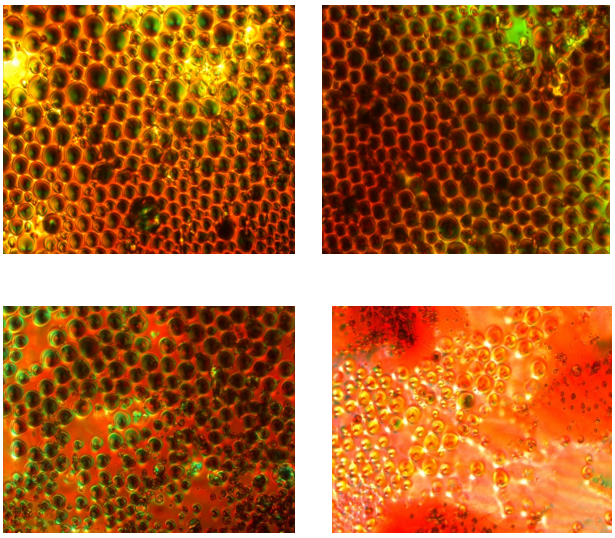

Fig. 5. Optical microscopic images in polarized light for 30:70 PMMA:DOPIMP (wt.%) on cooling (a) at 77 °C (b) 71 °C (c) 64,5 °C and (d) 52 °C

The optical textures of the polymer dispersed LC in the ratio 20:80 (wt.%LC) on cooling are shown in at 62 ^{0}C and 33 ^{0}C on cooling are shown in Fig. 6, respectively.

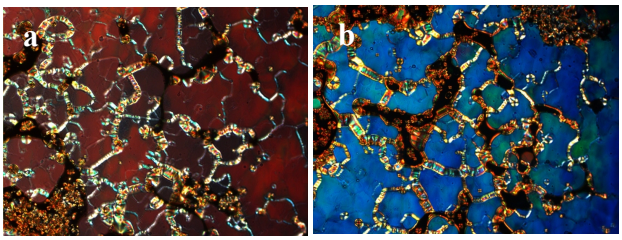

Fig. 6. Optical microscopic images in polarized light for 20:80 PMMA:DOPIMP (wt.%) on cooling (a) at 62 °C and (b) 33 °C

As seen in textures, the liquid crystal droplets were not observed on cooling from the isotropic liquid, however the colour of the reflected light changes from red via, brown and green to blue depending on the helical pitch which is induced by chirality in the tilted smectic phase. It is clear that liquid crystal is not homogeneously dispersed in the polymer matrix.

The droplets size and shape of LC in the PDLC composite films are significant factors for the electro-optical and dielectric properties. Solvent evaporation rate influences in the aggregation structure of the PDLC composite films. The slow evaporation rate gives rise to the formation of bigger sized LC droplets, whereas smaller LC droplets occur by the fast evaporation rate.

The SEM images of 30:70 wt.% PMMA:DOPIMP in Fig. 7 clearly shows that the DOPIMP liquid crystal droplets were dispersed homogeneously in the PMMA matrix. The shape and size of the droplets were uniform in the PDLC composite films.

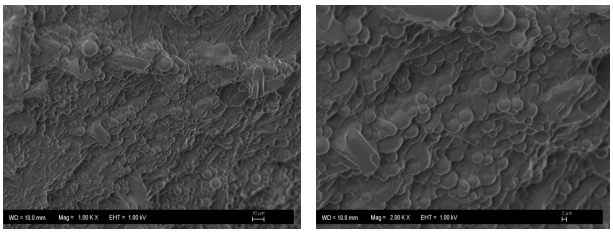

Fig. 7. SEM images of 30:70 wt.% PMMA:DOPIMP (a)20µm (b)1µm of dimensions composite films

4. Conclusions

The PDLC composite films were prepared from PMMA and calamitic liquid crystal DOPIMP by SIPS method with different compositions (wt./wt.%). The mesomorphic behavior of DOPIMP:PMMA composite films has been investigated by DSC and PM. The morphology of the films was studied using SEM and PM. The PDLC film with 30:70 wt.% PMMA:DOPIMP showed homogeneous distribution of phase separated DOPIMP liquid crystal droplets was clearly seen in optical microscopic and SEM images.

Acknowledgement

This research has been supported by Yıldız Technical University Scientific Research Projects Coordination Department. Project Number: 2013-01-02-KAP06. B. Bilgin-Eran is grateful to the Alexander von Humboldt Foundation, for financial support toward liquid crystal research.

References

[1] T. Y. Tsai, S. W. Lu, Y. P. Huang, F. S. Li, Journal of Physics and Chemistry of Solids **67**, 938 (2006).
[2] S. S. Parab, M. K. Malik, R. R. Deshmukh, Journal of Non-Crystalline Solids **358**, 2713 (2012).
[3] C. Provenzano, P. Pagliusi, G. Cipparrone, Opt. Express **15**, 5872 (2007).
[4] J. H. Ryu, Y. H. Choi, K. D. Suh, Colloids and Surfaces A: Physicochem. Eng. Aspects **275**, 126 (2006).
[5] P. Formentín, R. Palacios, J. Ferré-Borrull, J. Pallarés, L. F. Marsal, Synthetic Metals **158**, 1004 (2008).
[6] J. A. Jung, B. K. Kim, J. C. Kim, European Polymer Journal **42**, 2667 (2006).
[7] Y. J. Liu, X.W. Sun, Advances in OptoElectronics **2008**, 52 (2008).
[8] H. Ramanitra, P. Chanclou, B. Vinouze, L. Dupont, Molecular Crystals and Liquid Crstals **404**, 57 (2003).
[9] S. Coskun, B. Bilgin-Eran, O. Cankurtaran, F. Karaman, Journal of Optoelectronic and Biomedical Materials **1**, 91 (2009).
[10] J. Guo, M. Tang, H. Ling, L. Yuan, Materials Letters

91, 20 (2013).
[11] P. Kotakonda, I. Naydenova, R. Jallapuram, S. Martin, V. Toal, Journal of Optics A: Pure and Applied Optics **11**, 2 (2009).
[12] J. B. Nephew, T. C. Nihei, S. A. Carter, Review Letters **80**, 15 (1998).
[13] M. K. Malik, P. G. Bhatia, R. R. Deshmukh, Indian Journal of Science and Technology **5**, 10 (2012).
[14] S. S. Parab, M. K. Malik, R. R. Deshmukh, Journal of Non-Crystalline Solids **358**, 2713 (2012).
[15] F. Cakar, H. Ocak, B. Bilgin-Eran, O. Cankurtaran, Optoelectron. Adv. Mat. **7**, 667 (2013).
[16] D. Guzeller, H. Ocak, B. Bilgin-Eran, M. Prehm, C. Tschierske, J. Mater. Chem. C **3**, 4269 (2015).
[17] H. Ocak, B. Bilgin-Eran, C. Tschierske, U. Baumeister, G. Pelzl, J. Mater. Chem. **19**, 6995 (2009).
[18] B. Bilgin-Eran, H. Ocak, C. Tschierske, U. Baumeister, Liquid Crystals **39**, 467 (2012).
[19] B. Bilgin-Eran, C. Tschierske, S. Diele, U. Baumeister, J. Mater. Chem. **16**, 1136 (2006).
[20] A. Nesrullajev, B. Bilgin-Eran, Journal of Molecular Liquids **209**, 25 (2015).
[21] R. R. Deshmukh, M. K. Malik, Journal of Applied Polymer Science **108**, 3063 (2008).
[22] R. R. Deshmukh, M. K. Malik, J. Appl. Polym. Sci. **109**, 627 (2008).

*Corresponding author: kurtaran90@yahoo.com